

See discussions, stats, and author profiles for this publication at: <https://www.researchgate.net/publication/272146633>

Notes on the Black Mat Sediment, Mucuñuque Catchment, Northern Mérida Andes, Venezuela

Article in *Journal of Advanced Microscopy Research* · August 2011

DOI: 10.1166/jamr.2011.1071

CITATIONS

7

READS

70

5 authors, including:



William C. Mahaney

Quaternary Surveys

345 PUBLICATIONS 4,297 CITATIONS

[SEE PROFILE](#)



David Krinsley

University of Oregon

158 PUBLICATIONS 3,238 CITATIONS

[SEE PROFILE](#)



Volli Kalm

University of Tartu

92 PUBLICATIONS 1,404 CITATIONS

[SEE PROFILE](#)



Kurt Langworthy

University of Oregon

21 PUBLICATIONS 141 CITATIONS

[SEE PROFILE](#)

Some of the authors of this publication are also working on these related projects:



Electronic Properties and Structure of Functionalized Graphene [View project](#)



Younger Dryas Impact Hypothesis [View project](#)

Notes On The Black Mat Sediment, Mucuñuque Catchment, Northern Mérida Andes, Venezuela

W. C. Mahaney^{1,*}, D. H. Krinsley², V. Kalm³, Kurt Langworthy⁴, and J. Ditto⁴

¹Quaternary Surveys, 26 Thornhill Ave., Thornhill, Ontario, Canada, L4J1J4

²Department of Geological Sciences, University of Oregon, Eugene, Oregon, USA, 97403-1272

³Institute of Ecology and Earth Sciences, Tartu University, EE51014, Tartu Estonia

⁴CAMCOR, University of Oregon, Eugene, Or., USA, 97403

The enigmatic black mat sediment complex in the northern Andes, previously considered the product of a high-grade lightning strike and low grade brush fire, has been upgraded recently to a conflagration resulting from incoming asteroid/comet impact over the Laurentide Ice Sheet at approximately 12.9 ka. Previous evidence from the black mat beds of disrupted quartz and orthoclase grains and intense firing from incoming C-rich ejecta is further supported by new SEM/EDS and FIB analyses of fine grain silt and clay spherules (10~2 μm dia.) of C, Fe and Mn composition, a mixed material of partly ejecta and partly country rock. Because the environment at the time of ejecta impact was in the initial stage of seral vegetative development as wet tundra, part of the clay/organic balls, classic 'house of cards' form, which constitute a portion of the sediment complex, may be of cosmic origin. Evidence of cyanobacteria and fungal filaments on and within grain coatings are probably post depositional and therefore of terrestrial origin.

Keywords: Asteroid/Comet Impacts, Black Mat, Younger Dryas Glaciation.

1. INTRODUCTION

The Younger Dryas readvance of 12.9 ka has long been a mystery as to what perturbed the climatic warming of the Bølling-Allerød interstade to produce a worldwide readvance of ice. Although short-lived (~1 kyr) the YD has been linked to outflow of cold water into the Atlantic^{1,2} and a millennium long winter resulting from an asteroid or comet impact thought to have taken place over the Laurentide Ice Sheet;³⁻⁵ The exact place of breakup of the cosmic vehicle is unknown although suspicion centers on central Canada, perhaps over what is now Manitoba.⁶⁻⁸ Presumably the incoming bolide entered the Earth's atmosphere from the north, radially spreading ejecta in a wide dispersal pattern with interhemispheric proportions. That the impact was of high magnitude approaching extirminator proportions is supported by interhemispheric fallout and hypothesized extinction of Pleistocene megafauna and the demise of the Clovis culture^{4,5,9} Reversal of the Bølling/Allerød warming following the worldwide growth of ice during Isotope Stage 2 and sudden onset of the YD cooling (~12.9 ka) has been a seminal event of study for researchers over the last two to three decades.^{2,10}

Many workers have focused on the geomorphology and stratigraphy of the YD advance,¹¹⁻¹⁵ synchronization of paleoenvironmental events over wide areas¹⁶ and pollen chronologies and sequences.¹⁷ Still others focused strictly on dating moraines,¹⁸ concluding, from dated moraine surfaces falling within the YD window of ~12.9–11.9 ka, that the subject deposits actually resulted from glacial readvance. All this, despite the lack of conclusive moraine stratigraphic evidence to show overriding of weathered bedrock, older moraines, paleosols or bog sediments (discussion in Mahaney¹⁹ concerning unsuccessful attempts to uncover evidence to substantiate glacial readvance).

Correlating the YD event with the Clovis-Megafaunal extinction⁹ brings into question the impact of ecological disruption that may have occurred over wide areas of North and South America and Europe. While little is known of the European impact and its botanical effects, North American ecological disequilibrium is well studied.^{3-5,20} Given the presence of impact ejecta in the northern Andes, one which brecciated and carbonized glaciofluvial beds deposited by the retreating Allerød ice,^{21,22} ecological destabilization of the newly established wet tundra near the retreating ice was likely widespread. Similar ecological disruption of older surfaces

*Author to whom correspondence should be addressed.

in the lower Andean valleys, so far unreported, must have been of equal or greater magnitude.

2. YD EVENT: MÉRIDA ANDES

The YD event in the northwestern Venezuelan Mérida Andes occurs in two of the higher catchments between elevations of 3800 and 4050 m, the former in Mucuñuque Valley, the latter below the Humboldt Massif. The Mucuñuque Catchment (8° 47' N; 70° 49' W) details a stratigraphy that shows multiple glacier oscillations of the retreating Allerød ice culminating in a push moraine (Site MUM7) constructed presumably by the advancing YD ice, the exact date unconfirmed by radiocarbon dating since no biological materials were uncovered when the site was first mapped and deposits sampled in 1998.²³ Ages for the YD advance come from Site MUM7B, 300-m up valley from Site MUM7, where AMS ¹⁴C dates of 11440 ± 100, 11760 ± 80 and 11850 ± 180 yr BP yield calibrated AMS ¹⁴C ages of 13.8–13.4 and 14.1–13.3 ka cal BP at 235 cm depth and 13.5–13.3 ka cal BP at 232 cm depth. The material dated is alluvial peat and peat situated ~20 cm below the Mn–Fe–C encrusted pebbly beds that make up the black mat complex (Fig. 1(B)). Because the black mat bed has been demonstrated to be of cosmic origin^{22,24} one is forced to argue that the 20-cm thick beds of coarse sand,

stratified fine sand and fine alluvium account for all sediment emplaced over the millennium prior to the event that produced the black mat bed. With the lack of till in the section only the outwash beds above the black mat amount to the record left behind by the retreating YD glacier, at an unknown but postulated time of ~12 ka cal BP. The surface Regosol/Entisol (Fig. 1(B)), a Cryorthent,²⁵ has weathered *in situ* since the YD event. Lack of a B horizon in a soil with 1-m of precipitation and sufficient soil moisture for leaching is attributed to biogenic factors similar to what has been documented in the lower catchment.¹⁵

As depicted in Figure 1(B), deposit contacts are near planar and sharp suggesting erosion and possibly considerable truncation, all of which further poses the question of survival with the advancing YD ice only a short distance up valley. Tropical glaciers today¹⁹ are the warmest of the warm glaciers, constantly leaking water into bedrock, till, moraine and glaciofluvial sediment at their base. Even with a temperature depression of 6–8 °C during the ice ages, and perhaps somewhat less during the Late Glacial, sediment at ice/deposit contact was likely water soaked and hence pressure would be hydrostatic, i.e., the same in every direction. Without directed shear stresses the basal deposits would suffer only water saturation, the passage of ice inflicting little to nil damage on the sediment.²⁶

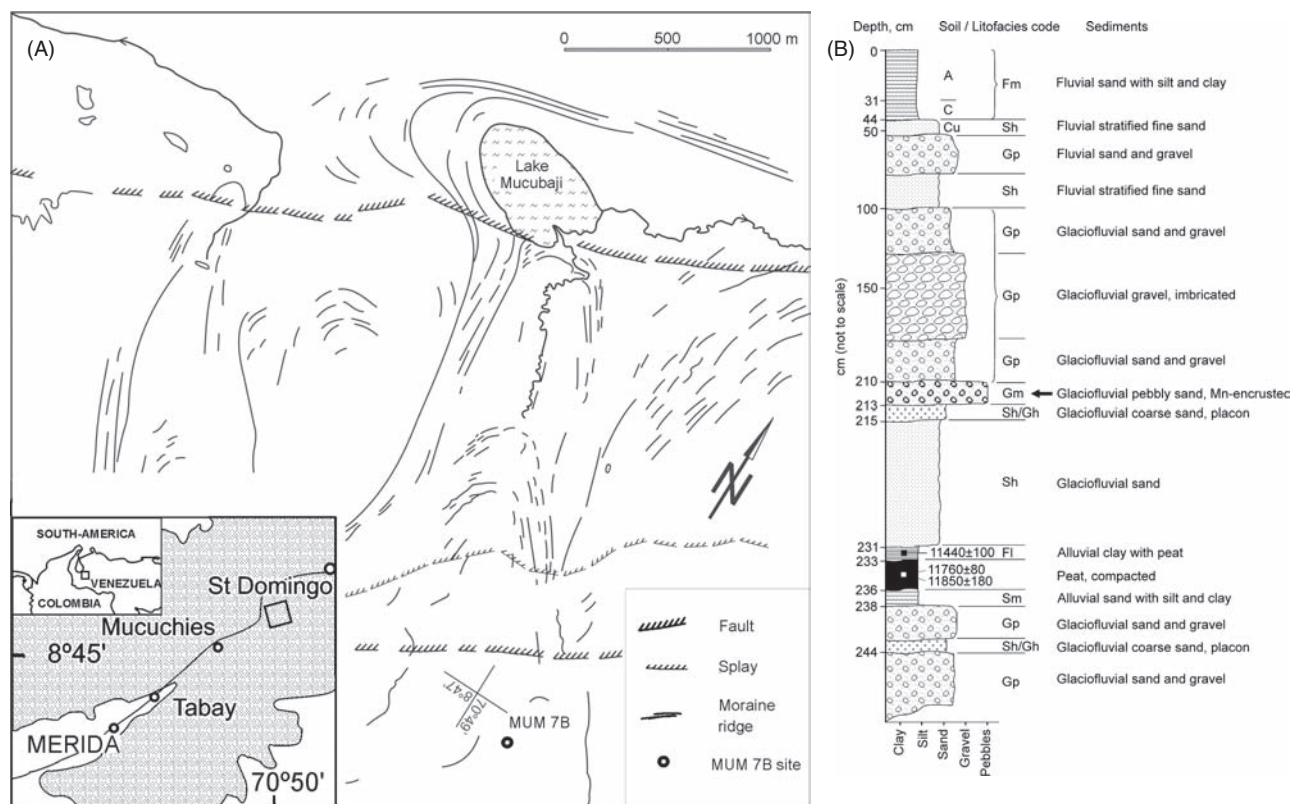


Fig. 1. (A) Map of the black mat site; (B) Stratigraphy of the MUM7B site.

3. REGIONAL GEOLOGY AND CLIMATE

The Mucuñuque Catchment (Fig. 1(A)) drains the north-western slope of the cordillera Sierra de Santo Domingo in the eastern cordillera of the Mérida Andes. The SW–NE oriented Mérida Andes extend from the Venezuelan–Colombian border to Barquisimeto and constitute a 100-km wide mountain belt with peaks reaching up to 5000-m in the central part of the chain. This belt began to rise in the late Miocene, probably as the consequence of the collision of the Panama arc against the South American plate.^{27–29} The NE-trending 500 km long Boconó fault longitudinally cross-cuts the Mérida Andes in its axial part. The Sierra de Santo Domingo and the Mucuñuque Catchment are located on the northeastern limb of the fault, on Precambrian bedrock of gneiss and granite of the Iglesias Group.³⁰

The SE–NW oriented Mucuñuque Catchment is a fault-controlled glacially-carved valley, descending from elevations above 4200 m on the western slopes of Pico Mifés (4600-m a.s.l.) and Pico Mucuñuque (4672-m a.s.l.). The Mucuñuque Valley debouches into Lago Mucubaji (ca. 3600-m a.s.l.) which is drained by Rio Santo Domingo into the Orinoco Basin. A number of transverse bedrock bars with waterfalls and ~100-m drop in elevation are spaced at the bottom of the valley below 4200-m. Cirques in the upper Mucuñuque Valley exhibit lagoons carved in bedrock or dammed by moraines.^{31,32} Within the valley upstream of the previously documented recessional moraines^{23,33} new investigations reveal surface moraine and outwash fans burying alluvial peat, which document a resurgence of ice corresponding to the YD.²³ The moraine/outwash complex of Late Glacial/Younger Dryas age, situated at 3800-m a.s.l. contains the sediments described in this report.

Today, the climate of the Mérida Andes is intermediate between the inner and outer tropics, with the majority of precipitation (ca. 935 mm annually) accumulating during boreal summer, and humidity is high year-round.³⁴ The mean annual temperature at the study area is approximately 10 °C.³⁵ There is little seasonal fluctuation in temperature although a 15–20°C diurnal fluctuation is normally experienced.

4. MATERIALS AND METHODS

The section, with a paleosol in the upper part, was excavated by hand and cleaned back 0.3 m to obtain a fresh face. Samples were collected for laboratory analysis and peats and clayey peats were collected for radiocarbon dating as explained by Mahaney and others.^{22,23} The ¹⁴C samples were collected with metal implements, air-dried in aluminum foil, kept frozen and sent for AMS dating within two-three weeks of collection. At the Iso-Trace Lab at University of Toronto, samples were washed with distilled water and acid treated to remove impurities and dated by

decay counting. Further treatment involved the application of hot 4N HCl, followed by extraction with 0.25N NaOH and acid washed again to remove possible carbonate and humic contaminants. Additional to this pretreatment, the clayey silt sample (TO-9278a) was demineralised in hot HCl and HF. All resulting dates were corrected for isotopic fractionation and calibrated with the OxCal v.3.10 calibration programme of Bronk Ramsey³⁶ using the INTCAL04 calibration data for the Northern Hemisphere.³⁷ The uncertainties of the ¹⁴C dates are reported as 1σ with the calibrated dates reported as 2σ. The calibrated dates are reported as the medians of the 2σ ranges.

Sediment and soil samples from the MUM7B section were air dried and selected samples subjected to oven drying at 110 °C to determine moisture content and calculate the air-dried equivalent of 50 g oven-dried sample. The air dried equivalent was used to calculate particle size following procedures outlined by Day.³⁸ Sands and silts separated by particle size analysis together with sands collected from encrustations on pebble clasts were subsampled and subjected to analysis by light microscope. Selected samples were then prepared as *t*-sections and/or mounted on stubs for analysis by SEM with secondary emission (Figs. 6–9) and Energy-Dispersive Spectrometry (EDS) following procedures outlined by Vortisch et al.³⁹ and Mahaney.⁴⁰ Samples were coated with C and tested against a carbon coated stub to estimate the spectral concentration. Determined elemental concentrations for the SEM images were based on calibrated standards. All other samples (Figs. 3–5) were imaged with the Focused Ion Beam (FIB) instrument.

5. RESULTS

The mixed mineral complex on a clast of quartz-biotite gneiss as shown on Figure 2 is representative of what the black mat looks like in the field. Moist colors range from 5YR 1.7/1 and 2.5YR 1.7/1, to 10R 4/8.⁴¹ As reported elsewhere (Mahaney and others,²⁴ XRD analysis of the encrusted material, subsampled from a number of coarse



Fig. 2. Light microscope image of black mat spherules on a local country rock clast.

clastic materials, depicts a composition of quartz, biotite, chamosite, and wuestite, the latter an Fe^{+2} oxide of native Fe often found in meteorites. Significant chlorite and illite are present intermixed with Mn oxides, the latter most probably a weathering product related to fluctuating redox conditions.

The light microscopic image shown in Figure 2 highlights the spread of spherules of glassy carbon across a Fe-rich and highly microlaminated surface. Encrusted C spherules are fixed randomly to the rock crystal matrix or welded onto a Fe–Mn substrate. Most often the C-rich spherules are observed welded onto the mineral matrix material.

Particle size analysis was determined from a collection of matrix sandy silt which amounts to <3% of the total weight of the black mat. The <2 mm fraction of the sample amounts to 83% sand, 14% silt and 3% clay based on the mean of three 25 g weight samples analyzed by dry sieving the sands followed by wet sieving the silt plus clay.

5.1. FIB Data

Imaging a surface section of black mat sediment with the FIB shows a typical surface area (Fig. 3(A)) of about $30 \mu\text{m} \times 30 \mu\text{m}$. The range of materials imaged include: C-rich spheres, other coated spheres, filamentous material interpreted to be fungi and uncoated clastic material of silt size. Numerous associated groups of C-rich spherules are found welded together as globules. Imaged filaments are coated with C and Fe + Mn and all are considered fossil. All resulting images are based on this area and on this one sample.

An enlarged area in Figure 3(B) at 5 k magnification shows individual microspherules of $\sim 2 \mu\text{m}$ diameter welded together. Tonal contrast may indicate C (dark) versus Fe (light) chemistries within each nodule. Enlargement (25 k) again of C-rich nodules (Fig. 3(C)) shows the porous character of individual microspheres, with others welded together and still others forming a melted 'thread' of nodules, or 'rod-like forms' from one welded group to another. The range of porosity to dense nodule form probably represents the temperature variability of incoming ejecta and differential cooling and condensation of CO_2 .

Further enlargement of the area in Figure 3(C) (Fig. 4(A)) to 65 k magnification provides additional details on the character of the fly ash material. Welded globules of C spheres, connected by 'rods,' are shown to be numerous within the black mat encrusted material. The same area (Fig. 4(B)), after liftoff of approximately $1\text{--}2 \mu\text{m}$ surface material with the Omniprobe, shows vertical slices through a fly ash 'house of cards' assembly which consists of a range of microspherules the size of individual clay minerals. The gash in the fabric is an artifact of moving the Omniprobe. Further increase

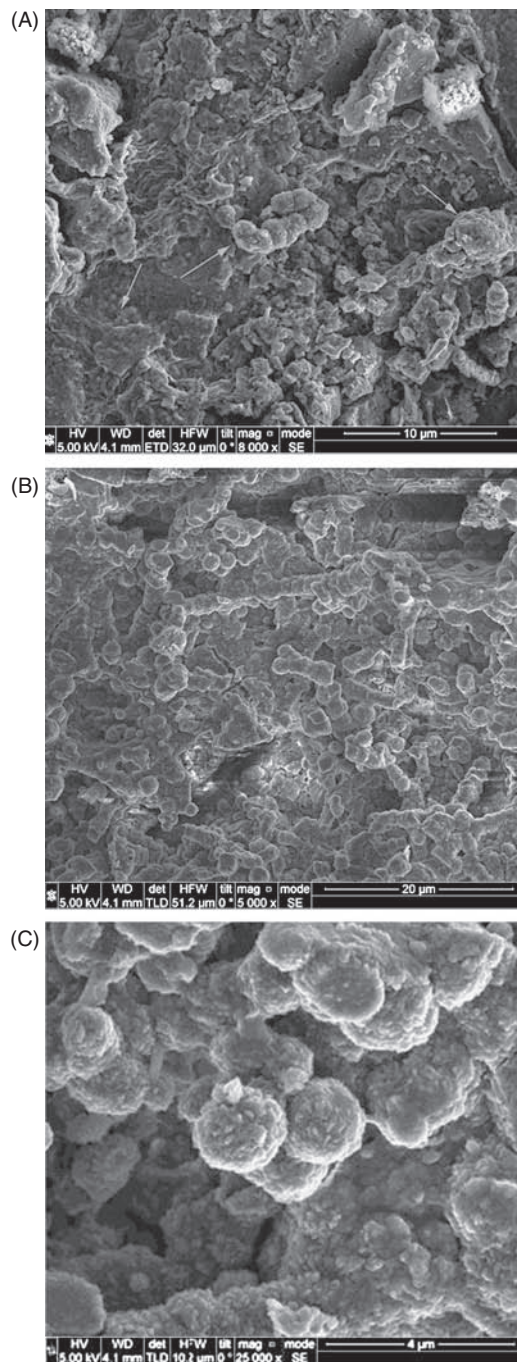


Fig. 3. (A) Top surface of black mat nodules at $8 \text{ k} \times$ magnification. Welded nodules (arrows) shown in several locations; (B) Enlargement of area in A at $5 \text{ k} \times$ magnification; (C) Small spheres (fly ash?), classic 'house of cards' constructed from incoming ejecta at 25 k magnification.

in magnification to 120 k magnification shows a range of microspherules from porous types to welded fine microforms. The large cavern at the top of the figure is an artifact created by the Omniprobe. Extreme magnification at 200 k magnification as in Figure 4(D) shows the porosity (upper right) and melted/condensed C material (upper left).

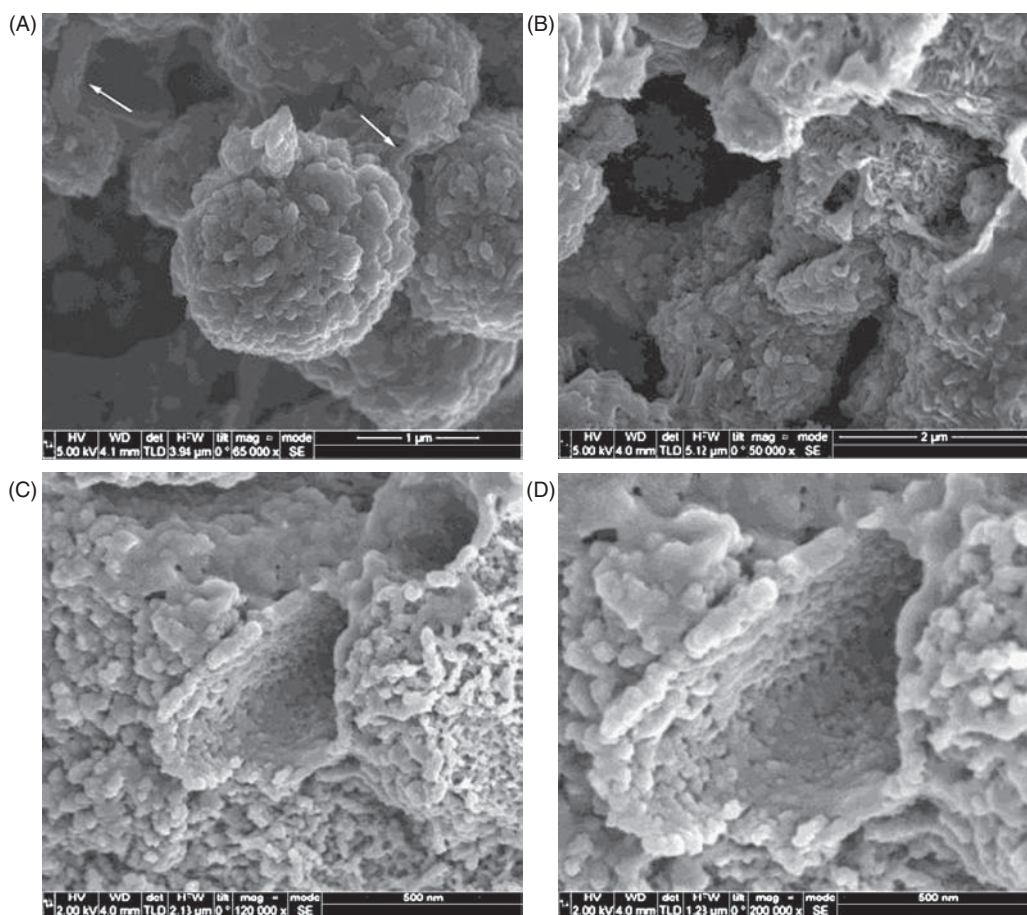


Fig. 4. (A) Enlargement of small welded spheres and small rods (arrows) at 65 k x magnification; (B) Area after liftoff with Omniprobe enlarged to 50 k x. Approximately 1 μm stripped off surface. The large tear near center is Omniprobe damage; (C) Uncoated area after stripping the surface with the Omniprobe. Enlargement at 120 k x; (D) Extreme magnification at 200 k x magnification of area in C.

Additional stripping into the Black Mat provides detailed character of a 3–4 μm deep area in the encrusted layer at 6500 \times (Fig. 5(A)). Microspherules of 1–2 μm diameter lie wedged within silt-size clasts of granitic and felsic gneiss. Globules of C-rich spheres are common along with near melted spheres. A long rod of intergrown microspherules of $\sim 2 \mu\text{m}$ diameter shown right of center is representative of melted C-rich material found in other black mat samples. Enlargement of the area in Figure 5(A) at 120 k magnification shows an exfoliated mass of welded microspherules, possible melted silicate grains (arrow) and a small quartz clast.

5.2. SEM/EDS

A range of light and heavy minerals (Fig. 6(A, B)) are found coated with C in the black mat. The filament with a diameter of $\sim 3 \mu\text{m}$ is at the high end of the fungi class of microorganisms but is well preserved in the sample. In this case welded orthoclase and magnetite are shown coated with Mn, P and C. The Ti is not sufficient for ilmenite and probably represents anatase, a weathering product.

A C-coated grain of probable sillimanite composition is shown in Figure 7(A). The filamentous material in Figure 6(A) is here shown in greater detail. The EDS spectrum shows C:Fe = 4:1 with some P present.

Occasional multi-coated fused Al microforms are found in the black mat as shown in Figure 8(A). The EDS spectrum comprises high C with considerable Co and F, both of which may be meteoric in origin.^{42,43} The Mn:Fe ratio of 3:1 is probably the result of fluctuating redox conditions in post depositional time.⁴⁴

Spherical microspherules such as shown in Figure 9(A) are common and typical of a classical ‘house of cards.’⁴⁵ This collection of microspherules of silt size dimensions is at the high diameter threshold, most welded globules are smaller.

6. DISCUSSION

The black mat bed described herein, situated some 16 cm above the radiocarbon dated beds, falls almost directly in line with the YD window. The sedimentation rate for sand lying between the YD dated beds and the black mat bed

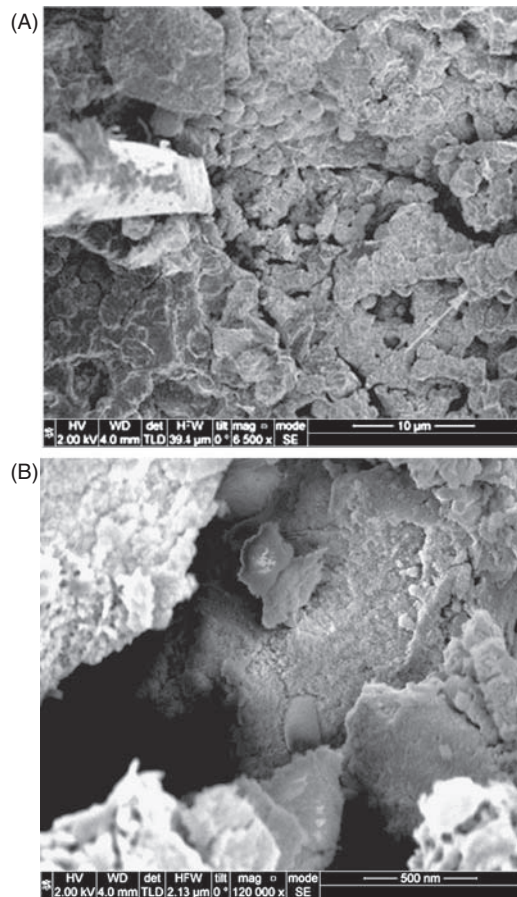


Fig. 5. (A) Three-4 μm area below surface stripped off with Omniprobe. Distorted 'house of cards' (arrow) and welded microspherules are in upper center and lower left areas. Magnification is 6.5 k \times ; (B) Enlargement of area in A at 150 k \times magnification.

is unknown; it may have been rapid or averaged out over a time span of a few hundred years. Taking the raw ^{14}C dates as a standard it required some ~ 400 yr to deposit the thick peat shown in the lower section; at one sigma the range is 280 yr and at two sigma 560 yr. While the lack of till makes the evidence for a YD origin somewhat circumstantial it is clear the lowermost extent of YD ice is at the 3800 m a.s.l. elevation, i.e., site MUM7, 0.25 km down valley. Less circumstantial perhaps, and certainly open to analysis and discussion, is the nature of the glassy C-rich spheres and microspherules, some open with considerable porosity and others welded together into globules and sometimes forming sheets of melted material, mostly C but often with considerable additions of Fe and other trace elements.

The light microscopic image in Figure 2 gives an impression of the random distribution of coating and globule distribution, the former more evenly distributed while the latter forms in groups presumably reflecting the distribution of heat across the impacting surface. What stands apart, forming the central point of analysis, is the classic 'house of cards' macro and microforms of C imaged

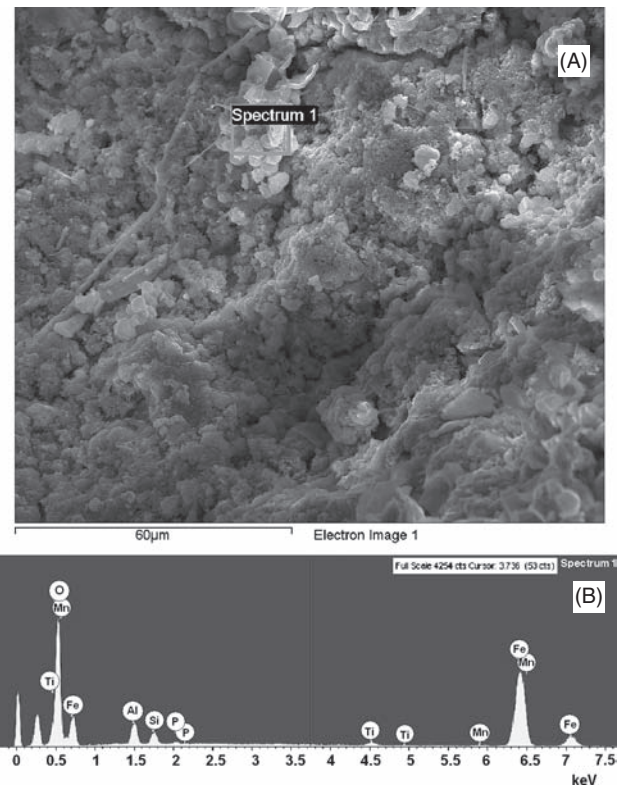


Fig. 6. (A) Selected area of C-coated welded grains (marked with spectrum bracket) of sillimanite and probable magnetite with very minor K-spar; (B) EDS spectrum depicts coatings of Mn, Ti, P and C (C is unlabeled).

with the FIB and supported with additional SEM imagery and EDS chemical analyses. Carbon, in all its forms in sediment complexes of all types and soil horizons, is not known to form the glassy spherules that are at the center-point of attention in the MUM7B bedform. Such microspherules are not known in normal alpine bog analyses, nor are they found in humic or argillic horizons in soils and paleosols, or in YD overrun peats or peats buried and deformed in older glaciolacustrine sediments.^{46,47} Spherules, as described herein, produced by combustion and similar to welding fume condensate, suggest very high temperatures followed by rapid cooling to produce the forms similar to common fly ash produced in incinerators and boilers (i.e., pleospheres). Coal is known to produce Si-rich glassy spherules with some S, Fe and K, products common in biomass incineration.⁴⁸

All reported rock firing events,^{49–53} whether caused by lightning or human agents, do not yield glassy, magnetic C spherules as documented here. Normal firing events leave rock spalls,⁵⁴ the amount of carbon fused to rock dependent upon the frequency of vegetation⁵³ but glassy microspherules are not observed. Smoke particulates, fibrous C films and fiber and charcoal are common residues resulting from forest and grassland fires⁵⁵

The identification of filaments in the imaged sample reflects the C-rich surface which supplied a source of

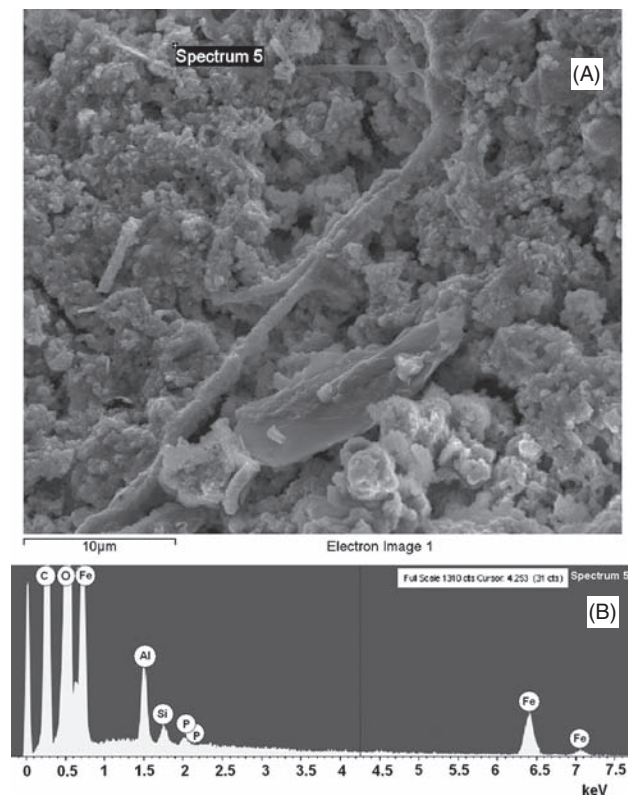


Fig. 7. (A) Coated sillimanite grain. Large coated filament in center with spatulate-form of carbonaceous material; (B) Coating of (C) Fe and P determined by EDS. Ratio of C:Fe = 4:1.

energy to microbes including bacteria previously imaged in the black mat bed.²³ The identification of bacteria relies almost exclusively on TEM analysis;⁵⁶ hence, no attempt was made to image even probable pseudomorphous bacterial colonies in this sample. Most of the filament forms thought to be fungi are found mainly embedded in Fe-rich material. Together with C as an energy source, and Fe necessary for respiration and water, all necessary components required for microbe proliferation are present. Thus, it is not surprising the black mat bed hosts considerable filament density.

Despite contrary hypotheses^{2,57} regarding the origin of black mat sediment, new sites and a considerable corpus of data continue to emerge and not just in North America. Among a variety of hypotheses put forth to explain this major perturbation in environmental conditions is: a major impact event in North America;^{4,5,9} breakup of *Comet Encke*⁶ and other possible impact craters such as one in southwestern Nova Scotia;⁵⁸ spring seepage and development of reducing environments⁵⁷ and changes in the thermohaline circulation of the North Atlantic.² All have been invoked to explain the black mat stratigraphic marker. However, given the evidence discussed here the cosmic hypothesis comes closest to explaining the glassy C-rich spherules, brecciated/impacted quartz and feldspar grains, fused metallic Fe and Al, presence of Cl as a possible inclusion in aluminosilicate glass⁵⁹ and occasional

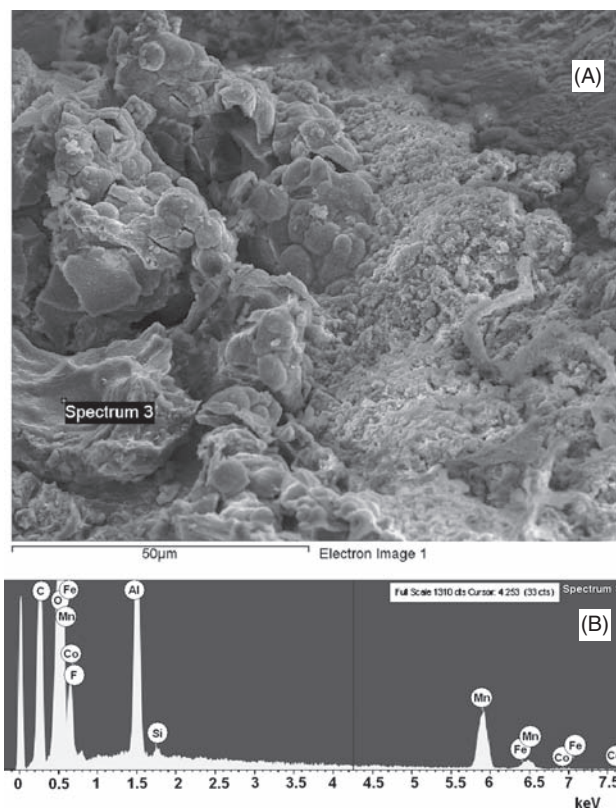


Fig. 8. (A) Multi-coated fused Al grain of medium silt size ~30 μm; (B) EDS spectrum shows (C) Co, F, Mn, Fe. Mn:Fe ratio = 3:1. Co and F could be by-products of impact ejecta.

Co and F within the black mat. The cosmic hypothesis deserves further testing.

The preliminary available database was compiled primarily from sites within the United States and Canada and centered on the presence of a ‘black mat’ stratigraphic marker dating to the climatic change at the Allerød/YD boundary. The theory argues for the breakup of a cosmic vehicle somewhere over the Laurentide Glacier at ~13 ka. The sediment within the ‘black mat’ at other sites comprises a thin layer of shocked sediment characteristic of ET impacts (not found so far at MUM7B), including but not limited to, glassy carbon and/or magnetic spherules, platinum group metals in fine silt, fragmental quartz, orthoclase, monazite and nanodiamond (lonsdaleite). Although clearly contentious as to proof for, and extraterrestrial origin of, the “black mat” Haynes,⁹ and Pinter and Ishman⁶⁰ argued against the theory citing a constant rain of cosmic materials that could occur without impact and fluctuating redox conditions that might yield Fe and Mn rich beds. However, the site location in the northern Andes described herein points tentatively to either an asteroid or comet event that reached far into South America, perhaps even to the southernmost tip of the continent and possibly to the Antarctic. Previously (Firestone and others^{4,5} and Mahaney and others^{21,22} argued for an asteroid impact but new evidence suggests the impact was cometary in nature.⁶

RESEARCH ARTICLE

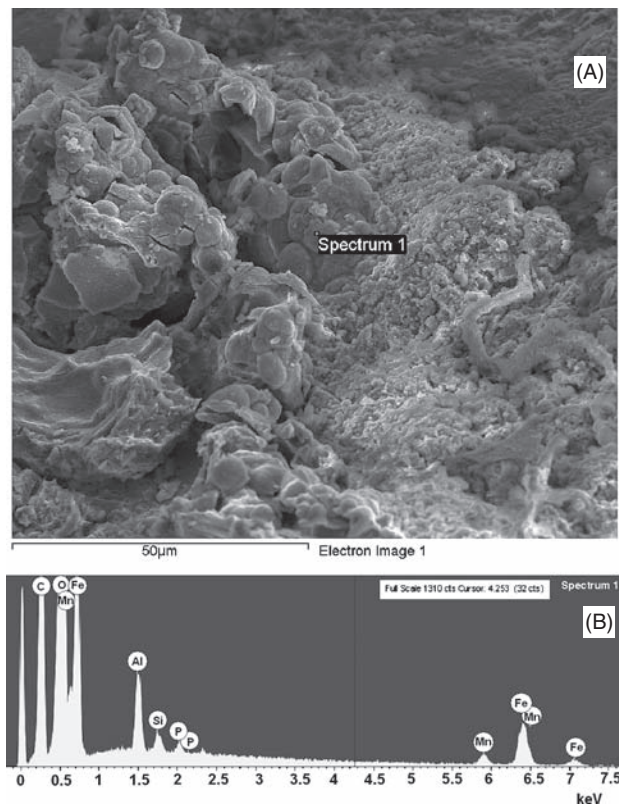


Fig. 9. (A) Near spherical fly ash, classical ‘house of cards,’ sphere at $\sim 8\text{--}10\ \mu\text{m}$ diameter is representative of clusters of C-rich spherules; (B) EDS shows high C and O, Al:Si = 3:1, low Fe and small amount of Mn and P.

The sheer magnitude of the proposed comet impact,⁶ an event so cataclysmic that remnants of the comet—the Taurid bodies which occupy near Earth orbits—would have caused a hemispheric-wide shock wave, a major perturbation introducing high-velocity ejecta into the atmosphere,⁵ fine ash reaching Venezuela at speeds up to 30 km/sec in less than 2 min. A strikingly high percentage of examined sites in N. America⁹ reveal a distinctive horizon of carbon-coated material (‘Black Mat’), which supports the theory despite hypotheses advanced for a different origin.^{21, 22} What remains unexplained with certainty at the MUM7B site is the origin of the carbon which clearly did not come from the minute or minimal vegetation complex in existence at time of ejecta impact. So, did all or part of the C come from an exploding carbonaceous chondrite or some mix of terrestrial and cosmic material?

7. CONCLUSIONS

The FIB imagery shown here illustrates the high resolution normal with this new instrumentation, especially the extreme high magnification that is possible. As illustrated with the classic ‘house of cards’ microspherules the variable character of the nodules can be seen ranging from porous individual spheres to globules of welded

microforms and to microspheres and rods of melted C-rich material, mixed occasionally with other chemical elements. While lacking key chemical and mineral evidence, specifically nanodiamonds and Ir, some platinum based metals (Ru and Rh) have been found in other specimens. Considering the great dispersal pattern from impact one would expect to sample a much greater mass of material to find lonsdaleite and any quantity of platinum metal (Ir) that might have a cosmic origin.

The glassy C-rich spherules and microspherules imaged and discussed here could be strictly terrestrial, cosmic, or a mix of terrestrial and extraterrestrial material. But, if a mix of both, certainly it is not expected that much C could be derived from a water soaked first-seral stage tundra forming in front of the receding Allerød ice mass in the Mucuñuque Valley. Compared with vegetation inhabiting the valley at 3800 m a.s.l., sparsely distributed *Polylepis* trees, with grasses and sedges, the ecosystem at 13.0 ka must have contained a lower count of distributed sedges, rushes and grasses with no timber. Ignition of the seral vegetation complex could not be expected to provide the copious amount of C found encrusted on the pebbly sand complex that constitutes the black mat at site MUM7B.

While it is likely that incoming ejecta blanketed the region, other sites similar to MUM7B have not been identified and black mat sediment has not been observed to occupy the contact between the YD and Late Glacial moraines (upper and middle till/moraine beds in MUM7). Incoming ejecta, encountering exposed bedrock, moraines and associated bogs, would not be expected to be long lived given the high erosion rates on steep slopes nor would the ejecta be easy to identify in organic-rich sections. Additional attempts need to be made to find stratigraphic sections similar to MUM7B or to search recovered cores from nearby lakes, especially the lakes in the lower Mucuñuque Catchment where black mat beds might be expected.

The welded character of the fired material, especially the glassy C-rich spherules, makes the encrusted material stand apart from Fe and Mn patinas common in placons (aquifers) in that it requires a much higher temperature to form, one that exceeds experimentally tested firing of quartz and feldspar. To achieve temperatures in excess of 900 °C, impacts capable of brecciating sediment and forming occasional inclusions of F and Co rich material suggests a cosmic origin for the enigmatic black mat bed.

Acknowledgments: This research was funded by Quaternary Surveys, Toronto.

References and Notes

1. J. T. Teller, D. W. Leverington, and J. D. Mann, *Quaternary Science Reviews* 21, 879 (2002).
2. W. S. Broecker, G. H. Denton, R. L. Edwards, H. Cheng, R. B. Alley, and A. E. Putnam, *Quaternary Science Reviews* 29, 1078 (2010).

3. D. J. Kennett, J. P. Kennett, J. G. West, J. M. Erlandson, J. R. Johnson, I. L. Hendy, A. West, B. J. Culleton, T. L. Jones, T. W. Stafford, Jr., *Quaternary Science Reviews* 27–28, 2530 (2008).
4. R. B. Firestone, A. West, J. P. Kennett, L. Becker, T. E. Bunch, Z. S. Revay, P. H. Schultz, T. Belgya, D. J. Kennett, J. M. Erlandson, O. J. Dickenson, A. C. Goodyear, R. S. Harris, G. A. Howard, J. B. Kloosterman, P. Lechler, P. A. Mayewski, J. Montgomery, R. Poreda, T. Darrah, S. S. Que Hee, A. R. Smith, A. Stich, W. Topping, J. H. Wittke, and W. S. Wolbach, *Proc. Natl. Acad. Sci. USA* 104, 16016 (2007).
5. R. B. Firestone, A. West, Z. Revay, T. Belgya, A. Smith, and S. S. Que Hee, American Geophysical Union Mtg. 07, PP41A sessions, San Francisco, AGU Annual Mtg, PP41A-02 (2007).
6. W. M. Napier, *Mon. Not. Royal Astron. Soc.* February (2010).
7. J. P. Kennett, L. Becker, and A. West, *AGU Annual Mtg, 2007*, PP41A-05 (2007).
8. D. J. Kennett, J. P. Kennett, A. West, C. Mercer, S. S. Que Hee, L. Bement, T. E. Bunch, M. Sellers, and W. S. Wolbach, *Science* 323, 94 (2009).
9. C. V. Haynes, *Proc. National Academy of Sciences* 105, 6520 (2008).
10. Z. Liu, B. L. Otto-Bliesner, F. He, E. C. Brady, R. Tomas, P. U. Clark, A. E. Carlson, J. Lynch-Stieglitz, W. Curry, E. Brook, D. Erickson, R. Jacob, J. Kutzbach, and J. Cheng, *Science* 325, 310 (2009).
11. P. W. Birkeland, D. T. Rodbell, C. D. Miller, and S. Short, *Boletín de Lima* 64, 55 (1989).
12. M. A. Reasoner, G. Osborn, and N. W. Rutter, *Geology* 22, 439 (1994).
13. G. Osborn, C. M. Clapperton, P. Thompson-Davis, M. Reasoner, D. T. Rodbell, G. O. Seltzer, and G. Zielinski, *Quaternary Science Reviews* 14, 823 (1995).
14. D. T. Rodbell and G. O. Seltzer, *Quaternary Research* 54, 328 (2000).
15. W. C. Mahaney, R. W. Dirszowsky, M. W. Milner, R. Harmsen, S. Finkelstein, V. Kalm, M. Bezada, and R. G. V. Hancock, *Journal of South American Earth Sciences* 23, 46 (2007).
16. J. J. Lowe, S. O. Rasmussen, S. Björck, W. Z. Hoek, J. P. Steffensen, M. J. C. Walker, and Z. C. Yu, *Quaternary Science Reviews* 27, 6 (2008).
17. T. Van der Hammen and H. Hooghiemstra, *Quaternary Science Reviews* 14, 841 (1995).
18. T. M. Shannahan and M. Zreda, *Earth and Planetary Science Letters* 177, 23 (2000).
19. W. C. Mahaney, Ice on the Equator, Wm Caxton Ltd., Ellison Bay, WI (1990), pp. 386.
20. A. Stich, G. Howard, J. B. Kloosterman, R. B. Firestone, A. West, J. P. Kennett, D. J. Kennett, T. E. Bunch, and W. S. Wolbach, Am Geophysical Union, PP13C-1471 (2008).
21. W. C. Mahaney, B. Kapran, M. W. Milner, V. Kalm, D. Krinsley, R. Beukens, S. Boccia, and R. G. V. Hancock, *Geomorphology* 116, 48 (2010).
22. W. C. Mahaney, D. H. Krinsley, and V. Kalm, *Sedimentary Geology* 231, 31 (2010).
23. W. C. Mahaney, M. W. Milner, V. Kalm, R. W. Dirszowsky, R. G. V. Hancock, and R. Beukens, *Geomorphology* 96, 199 (2008).
24. W. C. Mahaney, D. H. Krinsley, K. Langworthy, V. Kalm, A. Havics, K. Hart, B. Kelleher, S. Schwartz, P. Tricart, and R. Beukens, *Sedimentary Geology* 237, 73 (2011).
25. National Soil Survey Center (NSSC), Soil Survey Investigations Report No. 45. Version 1.00. USDA, Washington, DC (1995), pp. 305.
26. W. C. Mahaney, *Boreas* 24, 293 (1995).
27. B. De Toni, *Tectonics* 12, 13093 (1993).
28. B. Colletta, F. Roue, B. De Toni, D. Loureiro, H. Passalacqua, and Y. Gou, *Tectonics* 16, 777 (1997).
29. F. E. Audemard and F. A. Audemard, *Tectonophysics* 345, 299 (2002).
30. C. Schubert, *Quaternaria* 13, 225 (1970).
31. C. Schubert, *Zeitschrift für Gletscherkunde und Glazialgeologie* 8, 189 (1972).
32. C. Schubert, *Boreas* 3, 147 (1974).
33. W. C. Mahaney and V. Kalm, *Quaternary Surveys*, Toronto (1996), pp. 79.
34. A. Azocar and M. Monasterio, *Estudios Ecologicos en los Páramos Andinos*, edited by M. Monasterio, Ediciones de la Universidad de Los Andes, Merida, Venezuela (1980), pp. 207–223.
35. Servicio Meteorológico de la Fuerza, *Boletín Meteorológico del MANAR, Venezuela* (1975).
36. C. Bronk-Ramsey, OxCal Program v 3.10. Oxford, University of Oxford Radiocarbon Unit, <http://www.rlaha.ox.ac.uk/oxcal/oxcal.htm>. (2005).
37. P. J. Reimer, M. G. L. Baillie, E. Bard, A. Bayliss, J. W. Beck, C. J. H. Bertrand, P. G. Blackwell, C. E. Buck, G. S. Burr, K. B. Cutler, P. E. Damon, R. L. Edwards, R. G. Fairbanks, M. Friedrich, T. P. Guilderson, A. G. Hogg, K. A. Hughen, B. Kromer, G. McCormac, S. Manning, C. Bronk Ramsey, R. W. Reimer, S. Remmele, J. R. Southon, M. Stuiver, S. Talamo, F. W. Taylor, J. van der Plicht, C. E. Weyhenmeyer, *Radiocarbon* 46, 1029 (2004).
38. P. Day, *Methods of Soil Analysis*, edited by C. A. Black, American Society of Agronomy, Madison, WI (1965), pp. 545–567.
39. W. Vortisch, W. C. Mahaney, and K. Fecher, *Geologica et Paleontologica* 21, 245 (1987).
40. W. C. Mahaney, *Atlas of Sand Grain Surface Textures and Applications*, Oxford University Press, Oxford, U.K. (2002), pp. 237.
41. M. Oyama and H. Takehara, *Japan Research Council for Agriculture, Forestry and Fisheries*, Tokyo, Japan (1970).
42. D. E. Ames, J. Buckle, A. Davidson, and K. Card, Geological Survey of Canada, Open File 4570, Scale 1:50000 (2005).
43. D. Isvoranu and V. Badescu, *Journal of Cosmology* 2, 419 (2009).
44. K. H. Nealson, *Microbial Geochemistry*, edited by W. E. Krumbein, Blackwell, London (1983), pp. 191–221.
45. D. C. D. Nath, S. Bandyopadhyay, A. Yu, D. Blackburn, C. White, and S. J. Varughese, *Therm. Anal. Calorim.* 99, 423 (2010).
46. R. W. Dirszowsky, W. C. Mahaney, V. Kalm, M. Bezada, K. Hodder, *Journal South American Earth Sciences* 19, 526 (2005).
47. W. C. Mahaney, V. Kalm, B. Kapran, M. W. Milner, R. G. V. Hancock, *Geomorphology* 10, 99 (2009).
48. T. A. J. Kuhlbusch, *Environ Sci. Technol.* 29, 2695 (1995).
49. V. H. Barnett, *Journal Geology* 16, 568 (1911).
50. E. Blackwelder, *Journal of Geology* 35, 134 (1927).
51. D. Maki, *Geoarchaeology* 20, 449 (2005).
52. R. Grapes, *Pyrometamorphism*. Springer, NY (2006), pp. 276.
53. W. C. Mahaney, M. W. Milner, R. N. S. Sodhi, R. I. Dorn, S. Boccia, R. P. Beukens, P. Tricart, S. Schwartz, E. Chamorro-Perez, R. W. Barendregt, V. Kalm, R. W. Dirszowsky, *Geoarchaeology* 22, 797 (2007).
54. P. W. Birkeland, *Soils and Geomorphology*, Oxford University Press, Oxford, UK (1999), pp. 430.
55. E. V. Komarek, B. B. Komarek, B. B. and T. C. Carlyse, Misc Pub 3. Tall Timbers Research Station, Tallahassee, FL (1973).
56. H. Xu, T. Chen, Y. Jiang, Z. Nie, J. Liu, and Y. Wang, *Microscopy and Microanalysis* 9, 390 (2003).
57. J. Quade, R. M. Forester, W. L. Pratt, and C. Carter, *Quaternary Research* 49, 129 (1998).
58. G. Stevens, I. S. Spooner, J. Morrow, P. Pufahl, R. Raeside, R. A. Grieve, C. Stanley, S. Barr, and D. McMullin, American Geophysical Union, Fall Meeting, Abstract no. U23A-0854 (2008).
59. J. F. Stebbins and L.-S. Du, *American Mineralogist* 87, 359 (2002).
60. N. Pinter and S. E. Ishman, *GSA Today* 18, 37 (2008).

Received: 21 May 2011. Accepted: 13 June 2011.